Proceedings of the 3rd IFAC Workshop on Automatic
Control in Offshore Oil and Gas Production, Esbjerg,
Denmark, May 30 - June 1, 2018

Th_A_Regular_Talk.3

Control parings of a de-oiling membrane process

Kasper L. Jepsen [*] **Leif Hansen** [*] **Zhenyu Yang** [*]

[*] *Department of Energy Technology, Aalborg University, Esbjerg, Denmark*
(e-mail: klj, lha, yang@et.aau.dk).

Abstract: In offshore oil and gas productions increased attention is directed at the oil-water separation process, as environmental laws demand lower hydrocarbon concentrations in the discharged produced water. Membrane filtration is one possible candidate for significantly improving separation efficiency. However, fouling is one major challenge, where contaminants accumulate within the membrane and thereby adds additional flow resistance. This paper investigates the possibility of improving reference tracking and reducing fouling by improving control pairings and actuator placement. This is achieved by investigating the interaction between commonly deployed decentralized control loops on a membrane process model. The relative input-output interactions are evaluated across varying feed flow rates and membrane flow conductances to ensure that decoupling is maintained beyond the defined operating point. This work concludes that the location of the actuators affects the degree of decoupling significantly and to achieve the maximum degree of decoupling, different actuators must be selected across a variety of operating condition.

Keywords: Relative gain array, membrane, control parings, separation, multi-phase

1. INTRODUCTION

In the Oil & Gas sector large quantities of produced water are treated before discharge or reinjection. The treatment facilities typically consist of gas flotation, gravity-based separators, and hydrocyclones (Nel (2013); Coca-Prados and Gutierrez-Cervello (2011)). Current regulation for the North Sea allows water with less than 30 ppm oil-in-water (OiW) to be discharged (OSPAR-Commission (2012)), but increasing environmental concern and governmental regulation force new technology to be considered to improve separation efficiency. Membrane filtration is one potential technology that can improve separation efficiency and hence reduce discharged oil. Nonetheless, fouling (accumulation of contaminant in and on the membranes) of the membranes reduces the capacity and thereby increases the required installation size (Ashaghi et al. (2007), Webb et al. (2009), Silalahi and Leiknes (2009)).

There is a clear relationship between permeate flow (flux) and fouling rate. This relationship is described by Field et al. (1995), as "the critical flux hypothesis", which is experimentally observed by Wicaksana et al. (2012) and Howell (1995) and defined as: There exists a critical flux, at which below no fouling occurs and above fouling occurs. For many process systems a steady flow is required to ensure acceptable down- or up-stream operation. For produced water a steady feed flow rate is not guaranteed, as it is commonly affected by slugging (Pedersen et al. (2017)). Even under slugging, constant flux can be maintained by directing the flow to the permeate, rejection, or any combination of them.

For simple control design and to increase the robustness of the entire system, a decentralized control framework is often preferred in most practical applications. Although the commonly applied PID (proportional, integral, derivative) controller is widely deployed (Stoller and Mendes (2017), Busch and Marquardt (2007), Van Reis et al. (1997), Espinasse et al. (2002)), not much attention is given to short-term transient, tracking

performance, control structure, and only few mention the control pairings used (de Prada et al. (2014)). Typically, membrane filtration systems are controlled by maintaining either constant transmembrane pressure (TMP) or constant flux (Guo et al. (2012)). For produced water treatment, constant flux control is often deployed (Ashaghi et al. (2007), Silalahi and Leiknes (2009)).

A factor which has not been given much attention for efficient membrane filtration operations, is the placement of actuators. Placing actuators to minimize interactions between SISO control loops, could provide improved tracking of the reference and thereby avoid unnecessary fouling growth. Poor reference tracking causes the flux to occasionally exceed the reference flux. Exceeding the reference flux causes significantly larger fouling to build up, as the steady-state fouling resistance as a function of flux exhibits superlinear behavior.

In this paper a series of actuators and their placement will be considered and analyzed. This is achieved by deploying the Relative Gain Array (RGA) method to identify the optimal control pairings that minimize interactions between each SISO control loop. The analysis is based on the pilot-plant testing facility illustrated in Fig. 1. Interesting results show that optimal control pairings vary significantly across operating conditions.

The rest of this paper is organized as follows: Section 2 presents the considered configurations; section 3 presents the testing facilities; section 4 describe the process model; section 5 covers relative gain array method; section 6 defines the scenario which will be analyzed; section 7 presents the results; lastly, the paper is concluded in section 8.

2. OPERATIONAL CONFIGURATIONS

For this work, the configuration illustrated in Fig. 1 is chosen as the baseline and will be analyzed to determine which SISO control pairings would cause the least interactions between
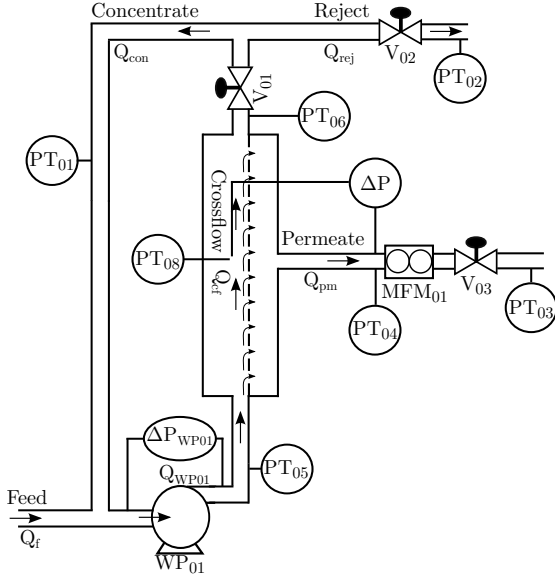
Fig. 1. Considered membrane filtration configuration.

control loops. The illustrated system is over actuated, meaning that not all actuators must be manipulated to maintain the system at the desired operating point.

For nominal operation of the filtration system, the produced water enters the crossflow loop through the feed flow and is then continuously circulated. The circulation or crossflow reduces the fouling build-up as shear rate dislodge oil from the membrane surface. The outflow from the membranes can be divided into two:

Permeate: Cleaner water is permeating the membrane leaving a higher OiW concentration in the crossflow loop.
Reject: A mixture, with higher OiW concentration than the feed, is directed away from the filtration system, either to be stored as waste or to be returned to previous separation step. The reject flow prevents the continuous accumulation of oil in the crossflow loop, that would otherwise completely foul the membrane Ashaghi et al. (2007).

A goal for any membrane filtration installation is to reach the desired operating conditions, typically represented by values of TMP, crossflow, reject, and permeate flow rates. This is typically achieved by installing the necessary actuators. Numerous actuator placement options exist and determining the optimal placement for dynamic control can be problematic, especially if cross couplings exist. The feed, permeate, and reject flow rates are restricted by the mass balance law, assuming non-compressible liquid and no buffer. Hence, only two degrees of freedom exist and a maximum of two variables can be independently controlled. The crossflow velocity (CFV) have no direct influence on mass flow balance, meaning it can be controlled separately. Considering the case where the feed flow is dictated by the upstream processes, where CFV and permeate flow rate are to be maintained, then theoretically only two correctly placed actuators are necessary, e.g. WP_{01} and V_{01}.

The considered system can be described with two uncontrollable inputs/disturbances, feed flow rate (Q_f) and fouling conductance (KV_f), and four actuators (V_{01}, V_{02}, V_{03}, and WP_{01}). Tab. 1 shows the generalized response of the system, e.g. a positive step for V_{01} results in higher crossflow and reject flow rate, and in less TMP and permeate flow rate.

Table 1. Generalized input-output tendency, when the respective input is increased

	Q_{cf}	ΔP	Q_{rej}	Q_{pm}
V_{01}	+	−	+	−
V_{02}	+	−	+	−
V_{03}	−	+	−	+
KV_f	−	−	−	+
Q_f	−	−	+	+
WP_{01}	+	+	−	+

3. TESTING FACILITY

The membrane filtration pilot plant is designed as an extension to the upstream experimental produced water treatment pilot plant, which includes horizontal pipeline, vertical riser, gravity-based separators, and hydrocyclones. The upstream produced water treatment pilot plant is described by Pedersen (2016).

The design criteria for the filtration system can be summarized as:

Flow capacity: The system is designed to handle an upstream flow of $3.5m^3/h$, such that operation in series is feasible.
High flexibility: The membrane filtration facilities are designed for research proposes and hence include adjustable configuration and additional sensors/actuators.
Anti fouling measures: The system is designed with both backwash and crossflow to provide fouling removal and prevention options.

4. PROCESS MODEL

Membrane filtration is often controlled with decentralized control and the interactions between the controllers are often ignored. To investigate the interaction a static model is formulated for the configuration illustrated in Fig. 1. The selected configurations are identical to possible configurations of the membrane filtration unit, as such the unit can serve as a basis for highlighting the potential interactions. The symbols used throughout this work are either presented in Fig 1 or explained in the text.

The flow at each intersection in the system can be formulated as in (1).

$$Q_{WP01} = Q_f + Q_{con}, \tag{1a}$$
$$Q_{con} = Q_{cf} - Q_{rej}, \tag{1b}$$
$$Q_{cf} = Q_{WP01} - Q_{pm}. \tag{1c}$$

The centrifugal pump is modeled as a controlled pressure source, which is dependent on the input (U_{WP01}) and the flow rate through the pump. With these assumptions, the pump can be described as (2).

$$\Delta P_{WP01}(Q_{WP01}, U_{WP01}) + PT_{01} = PT_{05}. \tag{2}$$

The flow through the valves is assumed to be highly turbulent, as such the flow is linearly proportional to the square root of the pressure drop over the valve. The flow coefficient for each valve depends on the given opening degree of the control valve. The three control valves in the system can be described as (3).

$$Q_{cf} = \sqrt{PT_{06} - PT_{01}} \cdot KV_{V01}(U_{V01}), \tag{3a}$$
$$Q_{rej} = \sqrt{PT_{01} - PT_{02}} \cdot KV_{V02}(U_{V02}), \tag{3b}$$
$$Q_{pm} = \sqrt{PT_{04} - PT_{03}} \cdot KV_{V03}(U_{V03}), \tag{3c}$$

where U_{Vxx} is the input for control valve no. xx, and $KV_{Vxx}(U_{Vxx})$ is the flow coefficient for control valve no. xx.

PT_{08} is considered a virtual sensor, but the pressure can be estimated according to (4a), under the assumption that the permeate flow rate is insignificant compared to the CFV. The TMP can be defined as (4b).

$$PT_{08} = \frac{PT_{05} + PT_{06}}{2}, \tag{4a}$$

$$\Delta P = PT_{08} - PT_{04}. \tag{4b}$$

Besides the three control valves, the system is significantly constricted by the crossflow and permeate channels. For crossflow and permeate flow rate the flow is assumed to be laminar, as such the flow rates are linearly proportional to the pressure drop over the restriction, as defined in (5).

$$Q_{cf} = KV_{cf} \cdot (PT_{05} - PT_{06}), \tag{5a}$$

$$Q_{pm} = KV_m \cdot \Delta P. \tag{5b}$$

where KV_{cf} is the flow coefficient for the crossflow channel, and KV_m is the combined flow coefficient for the permeate channels. The flow coefficients for the permeate channels are divided into two parallel parts: Firstly, the restriction caused by the narrow channels, which is considered constant. Secondly the restriction added by fouling, which is considered as an input disturbance. The combined membrane flow coefficient can be written as in (6).

$$KV_m = \frac{1}{\frac{1}{KV_{m|c}} + \frac{1}{KV_f}} \tag{6}$$

where $KV_{m|c}$ is the flow coefficient for a clean membrane, and KV_f is the flow coefficient for the fouling. The pressure drop in the transportation pipelines is ignored, as the constriction is assumed to be insignificant compared to the valves, crossflow, and permeate channels. The equations are solved for permeate, cross, and reject flow rates as well as TMP. The resulting function describes steady state values and is described as:

$$y = f(u, u_d), \tag{7}$$

where u, u_d, and y are defined as:

$$u = [U_{V01}, U_{V02}, U_{V03}, U_{WP01}]^T, \tag{8a}$$

$$u_d = [CV_f, Q_f]^T, \tag{8b}$$

$$y = [Q_{pm}, Q_{cf}, Q_{rej}, \Delta P]^T, \tag{8c}$$

where u_d is input disturbances, u system inputs, and y system outputs. The model is limited to steady-state relationships but can easily be extended to include valve and pump dynamics as well as hydrodynamics. These are not relevant for this study as it only considers steady-state analysis.

4.1 Model identification

The unknown elements that must be identified to carry out the analysis are:

- The control valves flow coefficient ($KV_{V01}(U_{V01})$, $KV_{V02}(U_{V02})$, and $KV_{V03}(U_{V03})$).
- The pump pressure boost function ($\Delta P_{WP01}(Q_{WP01}, U_{WP01})$).
- The flow coefficients (KV_{cf} and KV_m).

$\Delta P_{WP01}(Q_{WP01}, U_{WP01})$ is identify by running a series of steady-state experiments at different pump speeds and flow resistances. The experimental data are then used to identify a second order polynomial function. Additionally, identification experiments are carried out for each control valve, where
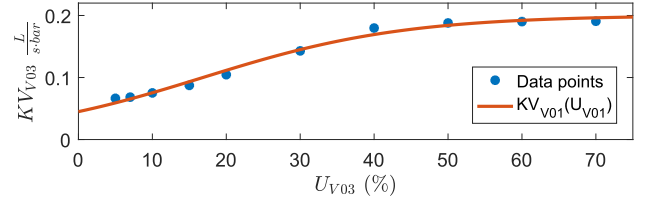

Fig. 2. Zoomed view of $KV_{V03}(U_{V03})$, note that $KV_{V03}(0) \neq 0$.

steady-state measurements of opening degrees, flow rates, and pressure drops through and over the valve are used to estimate the flow coefficient. The estimated flow coefficient, as a function of openings degree, is fitted to the function defined in (9);

$$KV_{Vxx}(U_{Vxx}) = \frac{1}{1 + e^{-a \cdot (U_{Vxx} - b)} \cdot c} \tag{9}$$

where, a, b, and c are tuning coefficients. Fig. 2 shows that above 50% opening the flow coefficient asymptotically approach a constant value. This is a consequence of identification experiment, where the valve is connected in series with $KV_{m|c}$, as the valve is opened the dominating flow resistance shift from the valve to the permeate channels. The series connection is unavoidable if the system is to be identified while assembled. The observed asymptotic behavior above 50% can indicate a potentially poor valve selection, as a valve smaller valve could have been selected without consequence.

Below 15% the flow coefficient curve seems to asymptotically approach a non-zero constant value. This could be caused by valve design, but the problem is tricky to investigate as the valve is unable to reliably achieve small degrees of opening. The valve should rarely be operated below 5% opening degrees, and if necessary the valve should be replaced with a smaller model. It was therefore chosen to accept the model deviation that occurs below 5%. The effect above 50% is of non consequence to the total system response, as the upper operating range is restricted by the series connected resistance.

The flow coefficient for the membrane crossflow channel is found based on experiments, and the constant flow coefficient through the permeate ($KV_{m|c}$) is estimated based on manufacturer's specifications. The model equations combined with the pump model are forming an implicit relationship, which is complicated to solve. A feasible solution was obtained by linearizing the pump model.

5. RELATIVE GAIN ARRAY

Relative Gain Array (RGA) is a method firstly described by Bristol (1966). The method provides a measure of interaction, between inputs and outputs, that is extensively used for pairing inputs and outputs in multi-loop control strategies. The RGA matrix is defined as (10).

$$\lambda(G(s)) = G(s) \times (G(s)^{-1})^T, \tag{10}$$

where $G(s)$ is the open loop gain matrix and $\times$ denotes element-by-element product. For non-square system, pseudo-inverse can be used.

The RGA-matrix can be evaluated across the frequency domain, where the crossover frequency is especially important for control design (Skogestad and Postlethwaite (2007)).While this does consider linear dynamic features, nonlinear features are

ignored. More commonly, the RGA analysis is often evaluated at steady state ($s = j\omega = 0$) to provide information about the systems steady-state behavior. For systems that operate across a wide range of operating conditions, linearization of the system may yield inaccurate results.

The RGA analysis in this work will be used to evaluate actuator placements, with the aim of minimizing the interaction between the decentralized control-loops. By iteratively evaluating the RGA matrix across different actuator placements and operating conditions, the actuator placement that results in the least interaction can be found. The analysis will consider two outputs (Q_{cf}, Q_{pm}), four inputs (U_{V01}, U_{V02}, U_{V03}, U_{WP01}), and changes in operating parameters (KV_f, Q_f), which results in a system with full row rank (i.e. has at least as many inputs as outputs). Given full row rank, the RGA-matrix is independent of output scaling but not input scaling (Skogestad and Postlethwaite (2007)), therefore all inputs are manually normalized between 0 and 1.

The open loop gain matrix of the non-linear system, defined in section 4, can be calculated according to (11).

$$G(u_0, u_{d0}) = \left.\frac{\partial f}{\partial u}\right|_{u_0, u_{d0}}, \tag{11}$$

where u_0 and u_{d0} are the operating point, and $G(u_0, u_{d0})$ is the open loop gain matrix, which is used to find the RGA matrix ($\lambda(G(u_0, u_{d0}))$). Interpretation of RGA matrix values are defined in Skogestad and Postlethwaite (2007). In general, large relative gain (RG), open-loop gain < closed-loop gain, indicates controllability problems, in terms the plant is difficult to control and have strong interactions. Preferred control pairings can be summarized as; the rearranged (preferred pairings on the diagonal) system should be as close as possible to the identity matrix. For this case, where extra inputs are considered, the usefulness for the extra inputs can be evaluated, if the column sum is very small ($\ll 1$), then one should consider removing the extra input.

Negative RG elements, where open-loop and closed-loop gains have different signs, should be avoided if possible. A negative element implies that an RHP-zero exists, and the RHP-zero can limit the performance of the final system. In addition, the RHP-zero combined with a traditional and often used PI-controller can cause system instability. In either case, negative RG elements should be avoided if it is desired to have Decentralized Integral Controllability (DIC) according to Theorem 10.6 in Skogestad and Postlethwaite (2007). DIC is often a desired system property, as it ensures that the system combined with integral action, remains stable even if controllers are taken out of action or inputs saturation occur. If negative RA elements cannot be avoided, total system can achieve stability, but inactivity from a controller can cause system instability, e.g. controller taken offline or input saturation.

6. SCENARIO DESIGN

The feed flow rate (Q_f) and the membrane fouling status (KV_f), can vary significantly during operation and therefore the RGA matrix is evaluated across variations in feed flow rate and membrane permeate conductance. As the model only have two degrees of freedom (see section 2) two actuators are selected. The combinations of selected actuators is one of the valves combined with the pump. Based on the selected valve,

Table 2. Designed operating conditions.

Parameter	Value
Q_f	$0.11\ L \cdot s^{-1}$
Q_{pm}	$0.1\ L \cdot s^{-1}$
Q_{cf}	$1.317\ L \cdot s^{-1}$ or $2m \cdot s^{-1}$
CV_f	$0.113\ L \cdot bar^{-1} \cdot s^{-1}$
Q_{rej}	$0.01\ L \cdot s^{-1}$

the required pump speed control valve's position is calculated, such that the required flow rates are maintained in steady state. The valves which are not selected remain fixed throughout the experiment. This procedure is iterated across all valves, different fouling conductances, and feed flow rates, where the variation are defined as:

Varying fouling conductance: The crossflow, permeate, reject and feed flow are fixed according to the values in Tab. 2. The two selected actuator inputs are then calculated to meet the flow requirements across the range $KV_f \in \{0.01, 0.2\}$, corresponding to a permeate flow of 0.01 to $0.161 L \cdot s^{-1}$, at a TMP of 1 bar.

Varying feed flow: The crossflow and fouling conductance are fixed according to the values in Tab. 2. The feed, permeate, and rejection flow rates are defined in (12), such that a constant permeate is kept while ensuring at least 30% rejection. Therefore, at low feed flow rate, the system is operated at a fixed rejection of 30%, while at higher feed flow rates the permeate flow rate is kept constant. This ensures that the system is never operated above 70% recovery or a permeate flux of $0.1\ L \cdot s^{-1}$. The two selected actuator inputs are then calculated as in the previous procedure.

$$Q_f \in [0, 0.35] \tag{12a}$$
$$Q_{pm} = min\{Q_f \cdot 0.7, 0.1\} \tag{12b}$$
$$Q_{rej} = Q_f - Q_{pm} \tag{12c}$$

7. RESULTS

The results presented in this section do consider the permeate flow rate and crossflow velocity as outputs. The results from the RGA analysis are shown in Fig. 3, 4, and 5. The figures show the RGA values for different operating conditions. Dashed lines are added to highlight the degree of valve opening at points of interest. The opening degree of the non-manipulated actuators are not identical across scenarios but are adjusted to achieve the widest possible operating range. The exact values are experimentally determined and written with each figure.

Scenarios with varying feed flow rates, especially Fig. 3a and 5a, have large variations in the RGA values, especially where the system switches between fixed recovery and permeate.

Crossing RGA values are also observed in Fig. 5b, where no transition between fixed recovery percentages and fixed permeate flow rate occur. The crossing is caused by the series connected permeate channel and valve, where a switch between the dominating resistance occurs. At low conductance, the available pressure is not sufficient to ensure permeate flow, as such the pump providing additional pressure is the best option. At high conductance the pressure is sufficient and V_{03} becomes the best option to control the permeate flow rate. Based on these results the following observations can be made for each of the following scenarios.

V_{01} scenario (Fig. 3):
Crossflow; V_{01} is providing the best decoupling. The dominances shift to WP_{01} at high and low feed flow rates.
Permeate; at rated conditions WP_{01} provides best decoupling. At low and high flow rates the preferred actuators are V_{01} and V_{02}, respectively.

V_{02} scenario (Fig. 4):
Crossflow and permeate; the RGA values are almost constant across varying conditions for the interval considered, which indicates that V_{02} and WP_{01} is a good combination to reduce nonlinear effects on the control pairings. However, the valid range of Q_f and KV_f is insignificant compared to other scenarios.

V_{03} scenario (Fig. 5):
Crossflow; the preferred pairing is with V_{01}, even across different feed flow rates and membrane flow conductance.
Permeate; optimal control pairing is not easily determined. At exactly the preferred operating condition WP_{01} provides the best parring. However, V_{03} provide better decoupling at boundary of feed flow rates, and higher membrane flow conductance.

8. CONCLUSION

This paper analyses the optimal control loop pairings according to the relative gain array method, across actuator placements, feed flow rate, and membrane flow conductance.

The scenario where V_{02} is chosen as the manipulated variable provides good decoupling. However, it was not possible to extend the operating range to include the desired operating conditions because it requires the valve to operate at nearly closed. Here the valve model is inaccurate and the valve is unable to reliably produce the small openings. Alternatively, the valve size could be reduced to provide better control at lower flow rates. The best decoupling, over a wider operating range, is achieved by deploying V_{01} and WP_{01} to control crossflow and permeate flow rate respectively. Over a reasonable range in Q_f and KV_f the most suited actuator for decoupling remains the same, which is not the case for the V_{03} scenario. The results show that no single actuator is superior across multiple feed flow rates and membrane flow conductance. A relatively poor degree of decoupling across operating conditions indicate that the filtration system could benefit from switching control, where the active controller is selected based on current conditions. Energy consumption of the actuators should be considered, as the energy usage varies significantly between pumps and valves. Additionally, MIMO control strategies, where actuators are coordinated, and interactions explored to achieve the desired results, could provide superior results.

Future work should include the scenarios where the pump is deselected, such that two valves are used for control. Furthermore, if the model dynamics can be formulated as a Hammerstein-Wiener model, the analysis can be extended to the frequency domain.

ACKNOWLEDGEMENTS

REFERENCES

Ashaghi, K.S., Ebrahimi, M., and Czermak, P. (2007). Ceramic ultra-and nanofiltration membranes for oilfield produced water treatment: A mini review. *Open Environmental Sciences*, (1), 1–8.

Bristol, E.H. (1966). On a new measure of interaction for multivariable process control. *IEEE Transactions on Automatic Control*, AC11(1), 133–134.

Busch, J. and Marquardt, W. (2007). Run-to-run control of membrane filtration in wastewater treatment - An experimental study. *IFAC Proceedings Volumes*, 40(5), 195–200.

Coca-Prados, J. and Gutierrez-Cervello, G. (2011). *Water purification and management*. Springer.

de Prada, C., Cristea, S., Mazaeda, R., and Palacín, L. (2014). Optimum operation of a beer filtration process. In H.G. Bock, X.P. Hoang, R. Rannacher, and J.P. Schlöder (eds.), *Modeling, Simulation and Optimization of Complex Processes - HPSC 2012*, 183–193. Springer International Publishing, Cham.

Espinasse, B., Bacchin, P., and Aimar, P. (2002). On an experimental method to measure critical flux in ultrafiltration. *Desalination*, 146(1-3), 91–96.

Field, R.W., Wu, D., Howell, J.A., and Gupta, B.B. (1995). Critical flux concept for microfiltration fouling. *Journal of Membrane Science*, 100(3), 259–272.

Guo, W., Ngo, H.H., and Li, J. (2012). A mini-review on membrane fouling. *Bioresource Technology*, 122, 27–34.

Howell, J.A. (1995). Sub-critical flux operation of microfiltration. *Journal of Membrane Science*, 107(1-2), 165–171.

Nel, T.S. (2013). An Introduction to Produced Water Management. Technical report.

OSPAR-Commission (2012). *North Sea Manual on Maritime Oil Pollution Offences*. OSPAR.

Pedersen, S. (2016). *Plant-Wide Anti-Slug Control for Offshore Oil and Gas Processes*. Aalborg Universitetsforlag. doi: 10.5278/vbn.phd.engsci.00183.

Pedersen, S., Durdevic, P., and Yang, Z. (2017). Challenges in slug modeling and control for offshore oil and gas productions : A review study. *International Journal of Multiphase Flow*, 88, 270–284.

Silalahi, S.H.D. and Leiknes, T. (2009). Cleaning strategies in ceramic microfiltration membranes fouled by oil and particulate matter in produced water. *Desalination*, 236(1-3), 160–169.

Skogestad, S. and Postlethwaite, I. (2007). *Multivariable feedback control: analysis and design*, volume 2. Wiley New York.

Stoller, M. and Mendes, R.S. (2017). Advanced control system for membrane processes based on the boundary flux model. *Separation and Purification Technology*, 175, 527–535.

Van Reis, R., Goodrich, E., Yson, C., Frautschy, L., Whiteley, R., and Zydney, A. (1997). ultrafiltration process control. *Journal of membrane science*, 130, 123–140.

Webb, C., North, C., Exploration, A., Nagghappan, L., and Water, V.N.a. (2009). Desalination of Oilfield-Produced Water at the San Ardo Water Reclamation Facility , CA. *Society of Petroleum Engineers*, (Figure 1), 1–21.

Wicaksana, F., Fane, A.G., Pongpairoj, P., and Field, R. (2012). Microfiltration of algae (Chlorella sorokiniana): Critical flux, fouling and transmission. *Journal of Membrane Science*, 387-388(1), 83–92.
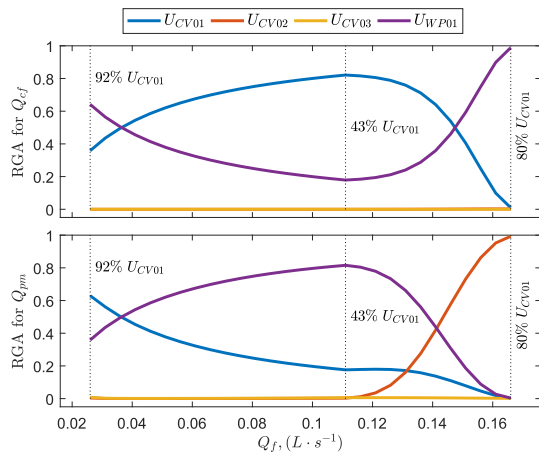
(a) RGA across varying feed flow (Q_f).
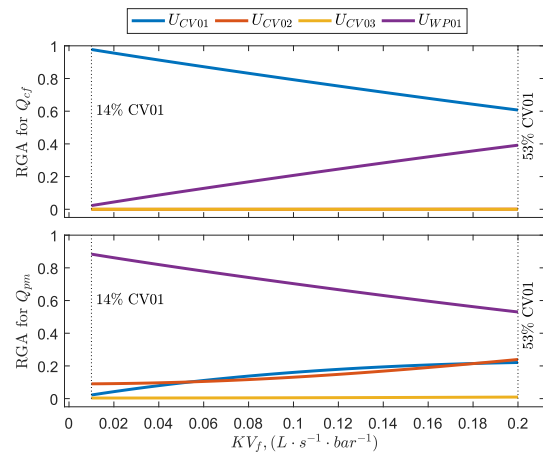
(b) RGA across varying membrane flow conductance(KV_f).

Fig. 3. Selected manipulated variables; U_{V01} and U_{WP01}. The remaining valves are kept constant at; $U_{V02} = 0.18$, $U_{V03} = 0.5$.
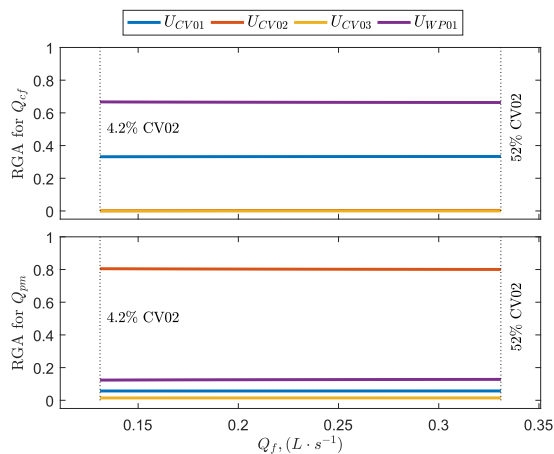

(a) RGA across varying feed flow (Q_f).
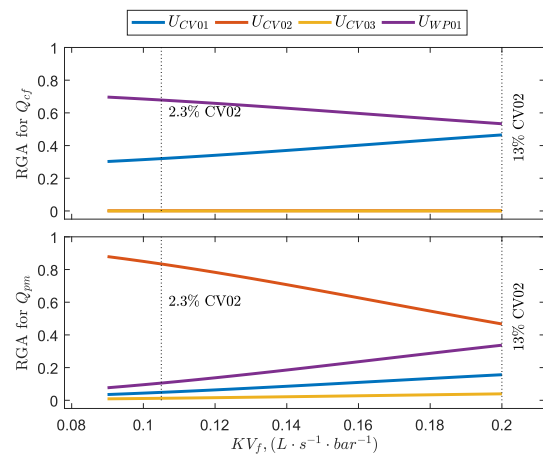
(b) RGA across varying membrane flow conductance(KV_f).

Fig. 4. Selected manipulated variables; U_{V02} and U_{WP01}. The remaining valves are kept constant at; $U_{V01} = 0.55$, $U_{V03} = 0.4$.
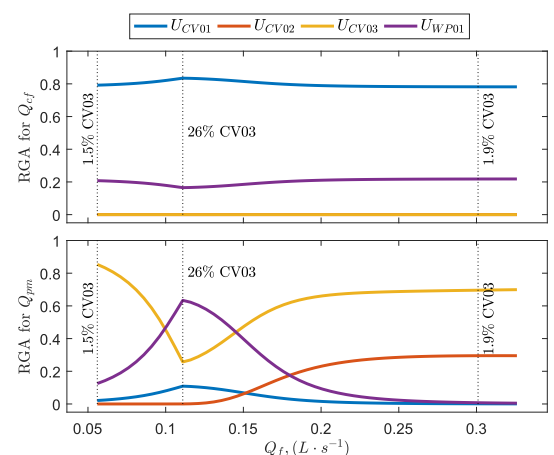
(a) RGA across varying feed flow (Q_f).
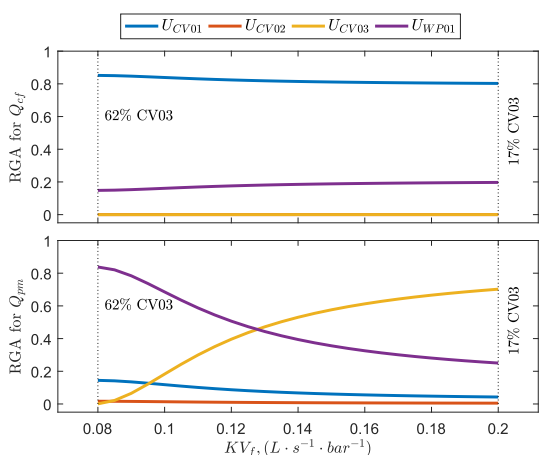
(b) RGA across varying membrane flow conductance(KV_f).

Fig. 5. Selected manipulated variables; U_{V03} and U_{WP01}. The remaining valves are kept constant at; $U_{V01} = 0.4$, $U_{V02} = 0.3$.